Received: 29 September 2021 | Revised: 20 July 2022 | Accepted: 08 August 2022

DOI: 10.1002/hep.32731

ORIGINAL ARTICLE

OPEN

Mitochondrial stress in advanced fibrosis and cirrhosis associated with chronic hepatitis B, chronic hepatitis C, or nonalcoholic steatohepatitis

Dimitri Loureiro[1,2] | **Issam Tout**[1,2] | **Stéphanie Narguet**[1,2] | **Cheikh Mohamed Bed**[1,2] | **Morgane Roinard**[1,2] | **Ahmad Sleiman**[1,2] | **Nathalie Boyer**[1,2] | **Nathalie Pons-Kerjean**[3] | **Corinne Castelnau**[1,2] | **Nathalie Giuly**[1,2] | **Dorothy Tonui**[1,2] | **Vassili Soumelis**[4,5] | **Jamel El Benna**[1] | **Patrick Soussan**[6] | **Richard Moreau**[1,2] | **Valérie Paradis**[1,2] | **Abdellah Mansouri**[1,2] | **Tarik Asselah**[1,2]

[1]Université Paris Cité, Centre de Recherche sur l'Inflammation, INSERM U1149, CNRS ERL8252, Paris, France

[2]Assistance Publique-Hôpitaux de Paris (AP-HP), Department of Hepatology, Hôpital Beaujon, Clichy, France

[3]Assistance Publique-Hôpitaux de Paris (AP-HP), Department of Pharmacy, Hôpital Beaujon, Clichy, France

[4]Université de Paris Cité, INSERM U976 HIPI Unit, Paris, France

[5]Assistance Publique-Hôpitaux de Paris (AP-HP), Laboratoire d'Immunologie et Histocompatibilité, Hôpital Saint-Louis, Paris, France

[6]Université de Paris Cité, INSERM U1135, Paris, France

Correspondence
Abdellah Mansouri, INSERM U1149, Centre de Recherche sur l'Inflammation, Faculté de Médecine site Bichat, 16 rue Henri Huchard, 75018 Paris, France.
Email: abdel.mansouri@inserm.fr

Tarik Asselah, Viral Hepatitis, INSERM UMR 1149, Hôpital Beaujon, 100 Boulevard du General Leclerc, 92110 Clichy, France.
Email: tarik.asselah@aphp.fr

Abstract

Background and Aims: Hepatitis B virus (HBV) infection causes oxidative stress (OS) and alters mitochondria in experimental models. Our goal was to investigate whether HBV might alter liver mitochondria also in humans, and the resulting mitochondrial stress might account for the progression of fibrosis in chronic hepatitis B (CHB).

Approach and Results: The study included 146 treatment-naïve CHB mono-infected patients. Patients with CHB and advanced fibrosis (AF) or cirrhosis (F3-F4) were compared to patients with no/mild-moderate fibrosis

Abbreviations: AF, advanced fibrosis; ALT, alanine aminotransferase; AST, aspartate aminotransferase; ATP, adenosine triphosphate; Bcl-2, B-cell lymphoma 2; BMI, body mass index; Bp, base pair; CHB, chronic hepatitis B; CHC, chronic hepatitis C; COX4I1, cytochrome *c* oxidase subunit 4I1; DAMPs, damage-associated molecular patterns; GGT, gamma-glutamyl transferase; HCC, hepatocellular carcinoma; HBV pgRNA, HBV pregenomic RNA; HBx, hepatitis B virus X protein; HSPA9, stress-70 protein, mitochondrial (heat shock protein family A [Hsp70] member 9; HSPD1, 60-kDa heat shock protein, mitochondrial (heat shock protein family D [HSPD1] member 1); iNOS, inducible nitric oxide synthase; LONP1, Lon peptidase 1; LPCR, long PCR; mDAMPs, mitochondrial damage-associated molecular patterns; MFN1, mitofusin 1; MFN2, mitofusin 2; MnSOD, manganese superoxide dismutase; MT-ATP8, mitochondrially encoded ATP synthase membrane subunit 8; MT-CO1, mitochondrially encoded cytochrome *c* oxidase I; MT-CO2, mitochondrially encoded cytochrome *c* oxidase II; mtDNA, mitochondrial DNA; ^{mt}UPR, mitochondrial unfolded protein response; nDNA, nuclear DNA; OPA1, mitochondrial dynamin-like GTPase (alias optic atrophy 1); OS, oxidative stress; PINK1, phosphatase- and tensin-induced kinase 1; PPARGC1α, peroxisome proliferator-activated receptor gamma coactivator 1 alpha; PRKN, parkin RBR E3 ubiquitin protein ligase (alias parkin, Parkinson juvenile disease protein 2); RNS, reactive nitrogen species; ROS, reactive oxygen species; TFAM, transcription factor A, mitochondrial; TOMM20, translocase of outer mitochondrial membrane 20; UTRN, utrophin (alias DRP1, dynamin-related protein 1).

Abdellah Mansouri and Tarik Asselah made an equal contribution

Supplemental Digital Content is available for this article. Direct URL citations appear in the printed text and are provided in the HTML and PDF versions of this article on the journal's website, www.hepjournal.com.

(F0-F2). Patients with CHB were further compared to patients with chronic hepatitis C (CHC; $n = 33$), nonalcoholic steatohepatatis (NASH; $n = 12$), and healthy controls ($n = 24$). We detected oxidative damage to mitochondrial DNA (mtDNA), including mtDNA strand beaks, and identified multiple mtDNA deletions in patients with F3-F4 as compared to patients with F0-F2. Alterations in mitochondrial function, mitochondrial unfolded protein response, biogenesis, mitophagy, and liver inflammation were observed in patients with AF or cirrhosis associated with CHB, CHC, and NASH. *In vitro*, significant increases of the mitochondrial formation of superoxide and peroxynitrite as well as mtDNA damage, nitration of the mitochondrial respiratory chain complexes, and impairment of complex I occurred in HepG2 cells replicating HBV or transiently expressing hepatitits B virus X protein. mtDNA damage and complex I impairment were prevented with the superoxide-scavenging Mito-Tempo or with inducible nitric oxide synthase (iNOS)–specific inhibitor 1400 W.

Conclusions: Our results emphasized the importance of mitochondrial OS, mtDNA damage, and associated alterations in mitochondrial function and dynamics in AF or cirrhosis in CHB and NASH. Mitochondria might be a target in drug development to stop fibrosis progression.

INTRODUCTION

Chronic hepatitis B (CHB) affects ~257 million persons worldwide, with a risk of advanced fibrosis (AF), cirrhosis, and HCC. In CHB, patients with AF or cirrhosis (Metavir score, F3-F4) should undergo surveillance because they are at risk of liver decompensation and HCC when compared to patients with no/mild-moderate fibrosis (F0-F2).[1–5]

Mitochondria play important roles in inflammation, innate immune, and antiviral responses, and both processes require healthy mitochondria.[6–10] Mitochondria-derived danger signals promote liver inflammation and directly activate hepatic stellate cells (HSCs) and drive the progression of liver fibrosis in mice and patients with NASH.[9]

The 16.5-kbp mitochondrial DNA (mtDNA) is double stranded circular DNA encoding critical subunits of the mitochondrial respiratory chain.[11] The mtDNA region between the origins of replication O_H and O_L is consistent with mutational and instability hot-spots regions.[12]

Unlike chromosomal DNA, mtDNA is more vulnerable to oxidative damage, because of its lack of protective histones and its attachment to the mitochondrial inner membrane, a main source of oxygen radicals in the cell.[13–15] Replication of oxidatively damaged mtDNA leads to point mutations and diverse mtDNA deletions that impair mitochondrial respiration in various liver diseases and progressive neurological disorders.[15,16]

Mitochondrial dysfunction and mitochondrial adaptive and protective mechanisms have been described in diverse chronic liver diseases.[7] These mechanisms include mitochondrial biogenesis, mitochondrial fission/fusion, mitochondrial unfolded protein response (^{mt}UPR), mitophagy, and induction of mitochondrial antioxidant capacities/pathways, all of which maintain mitochondrial homeostasis and ultimately cell survival.[7] Mitochondrial fusion is mediated by mitofusins 1 and 2 (MFN1 and MFN2) and mitochondrial dynamin-like GTPase (OPA1) whereas mitochondrial fission requires dynamin-related protein 1 (utrophin; UTRN).[7] Mitochondrial biogenesis maintains mitochondrial mass and is regulated by peroxisome proliferator–activated receptor gamma coactivator 1 alpha (PPARGC1α) and mitochondrial transcription factor A (TFAM). PPARGC1α and TFAM control the replication and transcription of mtDNA.[7] Defective mitochondria are cleared by Parkinson juvenile disease protein 2 (PRKN) and phosphatase- and tensin-induced putative kinase 1 (PINK1)-mediated mitophagy.[7]] ^{mt}UPR involves mitochondrial (HSPD1)/stress-70 protein, mitochondrial (heat shock protein family A [Hsp70]) member 9 (HSPA9) chaperones and Lon peptidase 1 (LONP1) peptidase, controls the stoichiometric balance between mitochondrial proteins encoded by the nuclear and mitochondrial genomes, ensures mitochondrial quality and proteases, and senses mitochondrial protein misfolding.[7]

The mitochondrial antioxidants include reduced glutathione (GSH) peroxidases, manganese superoxide dismutase (MnSOD), and peroxiredoxins.[7,17] Although mitochondria form large amounts of the superoxide radical anion, MnSOD accelerates its dismutation into hydrogen peroxide, which is detoxified into water by mitochondrial GSH peroxidases.[7,18] By decreasing superoxide steady-state levels, MnSOD limits the formation of reactive nitrogen species (RNS) such as peroxynitrite, a strong oxidant generated by the reaction of superoxide with nitric oxide (NO). MnSOD is inducible by reactive oxygen species (ROS) and cytokines, but it is inactivated by peroxynitrite.[7,18,19] Peroxynitrite and peroxynitrite-generated reactive intermediates can nitrate proteins and damage lipids and DNA and have been shown to be involved in mtDNA depletion.[18–20] In keeping with the role of inducible NO synthase (iNOS) in liver lesions, and the ability of MnSOD to decrease peroxynitrite formation, overexpression of MnSOD protected against liver mitochondrial oxidative stress (OS) in mice.[19]

In vitro and *in vivo* studies have shown that HBV or hepatitis B virus X protein (HBx) cause OS and alter mitochondrial dynamics and homeostasis.[7,8,10,21–27] HBV-induced OS might speed up the oxidative damage to mtDNA in patients with CHB. If this hypothesis is correct, one would expect massive oxidative damage to mtDNA in patients with CHB. The resulting mitochondrial dysfunction and associated alterations in mitochondrial dynamics would favor the progression of fibrosis in these patients. Conversely, AF and cirrhosis themselves might aggravate HBV-induced mtDNA damage and mitochondrial dysfunction. To verify this hypothesis, patients with CHB were compared to patients with NASH, chronic hepatitis C (CHC), and healthy controls. We provide here an association of these mitochondrial lesions with AF or cirrhosis in a large cohort of patients with CHB, NASH, and CHC. The possible underlying mechanisms of HBV- or HBx-associated mitochondrial OS, mtDNA damage, and mitochondrial dysfunction were further explored in human HepG2 hepato cells replicating HBV or expressing wild-type or mutated HBx protein *in vitro*.

PATIENTS AND METHODS

Patients and controls

One hundred ninety-one patients including 146 patients with CHB, 12 patients with NASH, 33 patients with CHC, and 24 patients with normal liver (hereafter designed as controls) were enrolled (Table 1, Figure S1). All patients' and controls' demographics and laboratory parameters were recorded at the time of the liver biopsy (LB).

Patients with CHB were eligible if they had been HBsAg-positive for ≥ 6 months before inclusion and were excluded if they had evidence of alcohol intake >20 g/d, coinfections, or NASH. Seventy-seven of 146 (53%) patients with CHB were HBeAg-positive chronic hepatitis (phase II), and 69 (47%) were HBeAg-negative chronic hepatitis (phase IV).

Patients with NASH or CHC were older than controls and patients with CHB ($p < 0.05$; Table 1). Patients with NASH also had higher body mass index (BMI) ($p < 0.001$), blood glucose ($p < 0.01$), and triglycerides ($p < 0.05$) than other groups. However, all the group patients and controls had comparable alanine aminotransferase (ALT) and aspartate aminotransferase (AST), but patients with CHB had lesser gamma-glutamyl transferase (ϒGGT; $p < 0.001$; Table 1).

LB specimens were formalin-fixed and paraffin-embedded. Sections (5 μm thick) were stained with hematoxylin and eosin, Mallory trichrome, Picrosirius red, and Perls and analyzed by a pathologist blinded to the clinical and laboratory data.

In patients with CHB and CHC, necroinflammation and fibrosis were assessed according to the Metavir scoring system.[3] Significant fibrosis was defined as Metavir score F3 or cirrhosis F4. Because patients with F3-F4 are at risk of HCC and liver decompensation when compared to patients with F0-F2, we stratified our patients in two groups regarding fibrosis grade: absent to moderate fibrosis (F0-F2) and AF or cirrhosis (F3-F4; Tables 1 and 2). Necroinflammation was graded as A0 to A3, and steatosis was assessed as the percentage of hepatocytes containing fat droplets (Table 1).

One hundred patients with CHB had F0-F2 and 46 had F3-F4 (Table 1, Figure S1). Similarly, 21 patients with CHC were with F0-F2 and 12 had F3-F4 (Table 1, Figure S1). All the 12 patients with NASH were with cirrhosis (F4; Table 1, Figure S1). No patient had cirrhosis decompensation or HCC. Only 12 (8%) of the 146 patients with CHB had important steatosis (> 33% of fat-engorged hepatocytes).

The 24 control liver specimens were obtained for diagnostic purposes and comprised percutaneous normal LB specimens obtained from 24 adults with mildly elevated serum ALT activity addressed to Beaujon Hospital (Clichy, France), in whom all causes of liver disease had been ruled out (medication, alcohol, chronic viral hepatitis, autoimmune processes, and metabolic disease; Table 1). In these control subjects, LBs were performed percutaneously under local anesthesia.[28] We selected liver samples on the basis of a histologically normal pattern: no portal or lobular inflammation and/or necrosis; absence of portal, central, or perisinusoidal fibrosis; and no other significant abnormal features (steatosis <5%, no iron overload, no ballooning or liver cell

TABLE 1 Characteristics of patients with CHB, CHC, NASH, and controls

	CHB	CHC	NASH	Controls
Total no. (*n*)	146	33	12	24
Sex (M/F)	92/54	14/19	6/6	13/11
Age, years (mean ± SEM)	41 ± 4	48 ± 7[b]	52 ± 15[b]	42 ± 10
BMI, kg/m^2 (mean ± SEM)	24.5 ± 3.3[f]	26.7 ± 4.4[d]	32.9 ± 7.7	23.1 ± 3.7[f]
ALT, IU/l (mean ± SEM)	111 ± 13	94 ± 41	102 ± 36	74 ± 37
AST, IU/l (mean ± SEM)	74 ± 14	60 ± 23	81 ± 45	51 ± 28
ϒGGT, IU/L (mean ± SEM)	79 ± 19[a]	133 ± 124	111 ± 103	198 ± 87[b]
Total cholesterol, mmol/l (mean, range)	4.4 (2.9–6.5)	4.7 (3.4–6.9)	4.6 (2.6–6.4)	3.9 (2.7–5.2)
Triglycerides, mmole/l (mean, range)	1.13[e] (0.38–3.69)	1.05[e] (0.47–2.15)	1.98 (0.77–5.50)	1.01[e] (0.43–1.39)
Glucose, mmole/l (mean ± SEM)	5.0 ± 0.6[d,c]	5.5 ± 1.1[a,b]	6.0 ± 1.2[a,b]	4.7 ± 0.3
Creatinin, µmol/l (mean ± range)	0.65 (0.34–1.34)	0.86[a,b] (0.59–1.25)	1.2[a,b,c] (0.80–1.68)	0.66 (0.58–0.82)
Albumin, g/l (mean ± SEM)	45 ± 7	45 ± 3	47 ± 4	43 ± 3
Platelets, 109/l (mean ± SEM)	174 ± 43	225 ± 48[b]	186 ± 50	271 ± 69
Virology				
HBeAg positive, *n* (%)	77 (53)	—	—	—
HBsAg (mean, $\log_{10}$IU/ml)	3.8	—	—	—
HBV DNA or HCV RNA, $\log_{10}$IU/ml (mean, range)	5.4 (2.2–8.2)	5.9 (5.0–7.1)	—	—
Liver histology findings				
Necroinflammatory activity				
A0 I A1 I A2 I A3	35 I 68 I 30 I 13	2 I 19 I 11 I 1	0 I 1 I 3 I 8	22 I 1 I 0 I 1
Fibrosis stage				
F0-F2 (*n*)	**100**	**21**	**0**	**24**
F0 I F1 I F2	26 I 40 I 34	1 I12 I8	0 I 0 I 0	23 I 1 I 0
F3-F4 (*n*)	**46**	**12**	**12**	**0**
F3 I F4	29 I 17	7 I 5	0 I12	0 I 0
Steatosis (*n*)				
≤5% of hepatocytes	118	16	0	21
5–33% of hepatocytes	16	9	1	3
>33–66% of hepatocytes	11	6	6	0
≥66% of hepatocytes	1	2	5	0

Note: For ALT level, the upper limit of normal was 34 IU/l in women and 45 IU/l in men. For AST level, the upper limit of normal was 31 IU/l in women and 35 IU/l in men. For GGT level, the upper limit of normal was 38 UI/l in women and 55 UI/l in men.
[a]Different from controls, $p < 0.05$.
[b]Different from CHB, $p < 0.05$.
[c]Different from CHC, $p < 0.05$.
[d]Different from NASH, $p < 0.05$.
[e]Different from NASH, $p < 0.01$.
[f]Different from NASH, $p < 0.001$; Mann–Whitney *U* test.

clarification, and no cholestasis or bile duct lesion). The 24 controls were all with no or minimal steatosis (<5% of fat-containing hepatocytes in 21% and 10% in 3; Table 1).

Study approval

The study was performed in accordance with the guidelines of the 1975 Declaration of Helsinki and the principles of Good Clinical Practice. All patients gave written consent, and the study was approved by the Ethics Committee of Beaujon Hospital (Département de la Recherche Clinique-Assistance Publique–Hôpitaux de Paris).

Analyses flow chart

Different amounts of DNA, RNAs, and/or proteins were obtained from distinct groups of patients and controls depending on the size of liver fragments that remained available after histological studies (Figure S1, Table 2; see Supporting Methods).

TABLE 2 Characteristics of patients with CHB and with mtDNA analysis, mRNAs, and/or protein assessment

	mtDNA Analysis		mRNA Assessment		Protein Assessment	
	n = 65		*n* = 104		*n* = 44	
	F0-F2	F3-F4	F0-F2	F3-F4	F0-F2	F3-F4
No. (*n*)	46	19	76	28	26	18
Sex, M/F (*n*)	32/14	10/9	61/15	20/8	18/8	10/8
Age, years (mean ± SEM)	42 ± 2	45 ± 5	40 ± 1	45 ± 2	41 ± 2	47 ± 3
BMI, kg/m^2 (mean ± SEM)	26.3 ± 2.3	24.5 ± 1.9	25.1 ± 0.6	24.5 ± 0.9	24.9 ± 0.9	23.7 ± 1.4
Serum levels at liver biopsy						
ALT, IU/l (mean ± SEM)	109 ± 22	112 ± 15	109 ± 15	121 ± 27	101 ± 21	72 ± 18
AST, IU/l (mean ± SEM)	75 ± 13	83 ± 13	75 ± 9	73 ± 12	82 ± 16	71 ± 19
GGT, IU/l (mean ± SEM)	88 ± 22	80 ± 15	76 ± 20	92 ± 17[a]	146 ± 53	56 ± 14
Total cholesterol, g/l (mean ± SEM)	0.8 ± 0.3	1.1 ± 0.2	0.9 ± 0.1	0.9 ± 0.2	0.7 ± 0.1	0.8 ± 0.3
Triglycerides, mmole/l (mean ± SEM)	1.0 ± 0.4	0.9 ± 0.3	1.2 ± 0.1	1.6 ± 0.2	1.7 ± 0.3	2.0 ± 0.8
Glucose, mmole/l (mean ± SEM)	4.8 ± 0.3	5.0 ± 0.3	4.9 ± 0.2	4.9 ± 0.3	5.4 ± 0.2	4.9 ± 0.2
HBsAg, $\log_{10}$IU/ml (mean ± SEM)	4.3 ± 0.2	5.0 ± 0.5	3.7 ± 0.1	4.6 ± 0.6	4.0 ± 0.2	4.8 ± 0.7
HBV DNA, $\log_{10}$IU/ml (mean ± SD)	4.7 ± 0.3	4.8 ± 0.6	5.5 ± 0.2	5.4 ± 0.4	4.8 ± 0.5	5.6 ± 0.9
Fibrosis stage						
F0	12	0	19	0	5	0
F1	21	0	40	0	14	0
F2	13	0	17	0	7	0
F3	0	10	0	17	0	12
F4	0	9	0	11	0	6

Note: RNA, DNA, and proteins were simultaneously obtained in 42 cases (31 with F0-F2 and 11 with F3-F4), and both DNA and proteins were obtained in 13 patients. The remaining 91 patients had only mRNA (64 cases), DNA (25 cases), or proteins (4 cases). For ALT level, the upper limit of normal was 34 IU/l in women and 45 IU/l in men. For AST level, the upper limit of normal was 31 IU/l in women and 35 IU/l in men. For GGT level, the upper limit of normal was 38 UI/l in women and 55 UI/l in men.

[a]Different from F0-F2, $p < 0.01$; Mann–Whitney *U* test.

Detection and sequencing of mtDNA deletions

Liver DNA was isolated as described.[15,16] The instability hot-spot mtDNA region (6080 bp) extending from nucleotides 8167 to 14,246 was screened by long PCR (LPCR) for the presence of mtDNA deletions. DNA samples from controls and patients with CHB or NASH were subjected to LPCR with primers A-B (Table S1), which concomitantly amplify undeleted and deleted mtDNA in a single reaction. The A and B primers coamplify a long fragment of 6080 bp from the undeleted mtDNA template and smaller fragment(s) from deleted mtDNA molecules, whenever present. The LPCR program included 30 cycles of 95°C for 45 s, 61°C for 10 s, and 68°C for 8 min and a final extension at 68°C for 7 min. LPCR products were analyzed on 1.5% agarose gels stained with SYBR Safe DNA intercalating agent, and DNA bands were detected by fluorography.

LPCR products were sequenced to determine the exact sizes and boundaries of the detected mtDNA deletions. mtDNA bands were excised from the gel, placed on the filter of a Spin-X Centrifuge Tube Filter, frozen at −20°C, and recovered by centrifugation. One hundred nanograms of the recovered product were then subjected to a single primer PCR sequencing reaction using the BigDye Terminator v3.1 Cycle Sequencing Kit and either primer C or D (Table S1). After heating to 94°C for 2 min, the reaction was cycled as follows: 25 cycles of 30 s at 94”C, 30 s at 55”C, and 4 min at 60°C. After removal of unbound dye terminators, samples were loaded on an Applied Biosystems 373A sequencer and run for 12 h on a 6% denaturing acrylamide gel.

Slot blotting and Southern blotting hybridization

Slot blotting was used to quantitate mtDNA and nuclear DNA (nDNA). Hepatic DNA (100 ng) samples from controls and patients with CHB or NASH were blotted onto a Hybond-N1 nylon membrane and hybridized with a 6080-bp probe that was generated by LPCR and αP^{32}dCTP-labeled by random priming. Membranes were stripped and hybridized with a human C_0t-1 nDNA probe, as described, and[29] mtDNA and nDNA were assessed by densitometry analysis of autoradiographs.

Proportions of mtDNA in its supercoiled, circular, and 16,569-bp linear forms were analyzed by Southern blotting using a human mtDNA specific-radiolabeled probe.[29] Liver DNA (1.5–3.0 μg) was loaded on 0.7% agarose gels without DNA intercalating labeling agents. Electrophoresed DNA was transferred to a Hybond-N1 nylon membrane and hybridized with the α-dCTP^{32}-labeled 6080-bp human mtDNA probe. The mtDNA forms were quantitated by densitometry of autoradiographs.

Real-time RT-qPCR assessment for liver mRNA levels, liver adenosine triphosphate determination, and western blotting analysis

RT-qPCR, liver adenosine triphosphate (ATP) determination and western blotting were performed also in our patients and controls (see the Supporting Methods section). Moreover, mitochondrial stress was investigated in HepG2 cells replicating HBV or expressing wild-type or mutated HBx proteins *in vitro* (Supporting Methods).

Statistical analysis

Data are expressed as mean ± SD. Categorical variables are expressed as absolute and relative frequencies. Statistical analyses were performed using GraphPad Prism software (version 9.0.1; GraphPad Software Inc., La Jplla, CA). The Mann–Whitney U test was used to assess differences between means. The chi-square (κ^2) or chi-square corrected for continuity (κc^2) tests were used to assess differences between frequencies. The Pearson method was used to assess the correlation between numerical variables. Patients with CHB, CHC, or NASH were compared to controls. Patients with F3-F4 were compared to those with F0-F2 within each group of patients and between these groups. The *n* values for each experiment are indicated in the figure legends. Significance was set up at $p < 0.05$.

RESULTS

mtDNA deletions in patients with CHB or NASH

mtDNA deletions were examined by LPCR and characterized by sequencing. In addition to the expected 6080-bp fragment amplified from undeleted mtDNA, the hepatic DNA from patients with CHB and patients with NASH gave amplification products of smaller lengths corresponding to diverse mtDNA deletions (Figure 1A,B). To determine the exact position of these rearrangements, these mtDNA bands were sequenced (Figure S2).

Four different 5385-, 4977-, 4881-, and 2451-bp mtDNA deletions, all flanked by direct repeats, were observed in these patients (Figure S2A).

The 4977- and 5385-bp deletions start within the gene for subunit 8 of ATP synthase (MT-ATP8), and the 4881-bp deletion starts within the gene for subunit 3 of cytochrome *c* oxidase (MT-CO3, complex IV; Figure S2A,B). The three deletions then involve the genes for subunit 6 of ATP synthase, MT-CO3, subunits 3, 4L, 4, and 5 of NADH dehydrogenase (complex I), as well as the interspersed genes encoding tRNA-His, tRNA-Gly, tRNA-Arg, tRNA-Ser, and tRNA-Lys (Figure S2B).

The 2451-bp deletion starts within subunit 3 of the NADH dehydrogenase gene and affected the genes for subunits 4, 4L, and 5 of complex I and tRNA-Tyr, tRNAs-Arg, tRNA-His, tRNA-Ser, and tRNA-Leu (Figure S2A,B).

The common 4977-bp deletion was observed in 46 (71%) of 65 patients with CHB and in 7 (58%) of the 12 patients with NASH and cirrhosis, but only in 5 (21%) of the 24 controls (Table S3). The 2451-bp deletion was detected in 9 of 19 (47%) patients with F3-F4 and in 12 of 46 (26%) with F0-F2, but in none of the patients with NASH nor in controls. The 4881- and 5385-bp deletions were respectively observed in 5 and 2 patients with CHB and F3-F4, but in none of the patients with CHB and F0-F2, NASH, or in controls (Table S3).

Considering all the four deletions, 56 patients with CHB (86%), but only 5 of 24 controls (19%), carried at least one mtDNA deletion ($\kappa^2 = 34.68$, $p < 0.005$; Table S3). The difference in the prevalence of mtDNA deletions persisted when patients with CHB and F3-F4 were compared to patients with CHB and F0-F2. Whereas 18 of 19 (95%) patients with CHB and F3-F4 exhibited at least one mtDNA deletion, only 30 of 46 (65%) patients with CHB and F0-F2 carried a single mtDNA deletion ($\kappa^2 = 20.04$, $p < 0.005$), and 1 patient harbored two distinct deletions. Two of the patients with F3-F4 had two concomitant deletions, and 2 exhibited three concurrent deletions (Figure 1A).

Compared to controls, prevalence of the 4977-bp deletion was significantly higher in patients with NASH and cirrhosis. Whereas 7 (58%) of 12 patients with NASH and cirrhosis exhibited the 4977-bp deletion, only 5 of 24 controls (19%) carried this common deletion ($kc^2 = 5.06$, $p < 0.025$; Table S3).

Similarly, the difference in prevalence of the 4977-bp deletion persisted when patients with CHB and F3-F4 were compared to patients with NASH and cirrhosis. Whereas 18 of 19 (95%) patients with CHB and F3-F4 exhibited at least one mtDNA deletion, only 7 of 12 (58%) patients with NASH and cirrhosis carried a single mtDNA deletion ($k^2 = 6.93$, $p < 0.005$; Table S3). This difference persisted even when only patients with CHB and cirrhosis were compared to patients with NASH and cirrhosis (i.e., patients with CHB and F3 were excluded from the analysis).

The 5 patients with CHB exhibiting two or three different mtDNA deletions were those with the highest

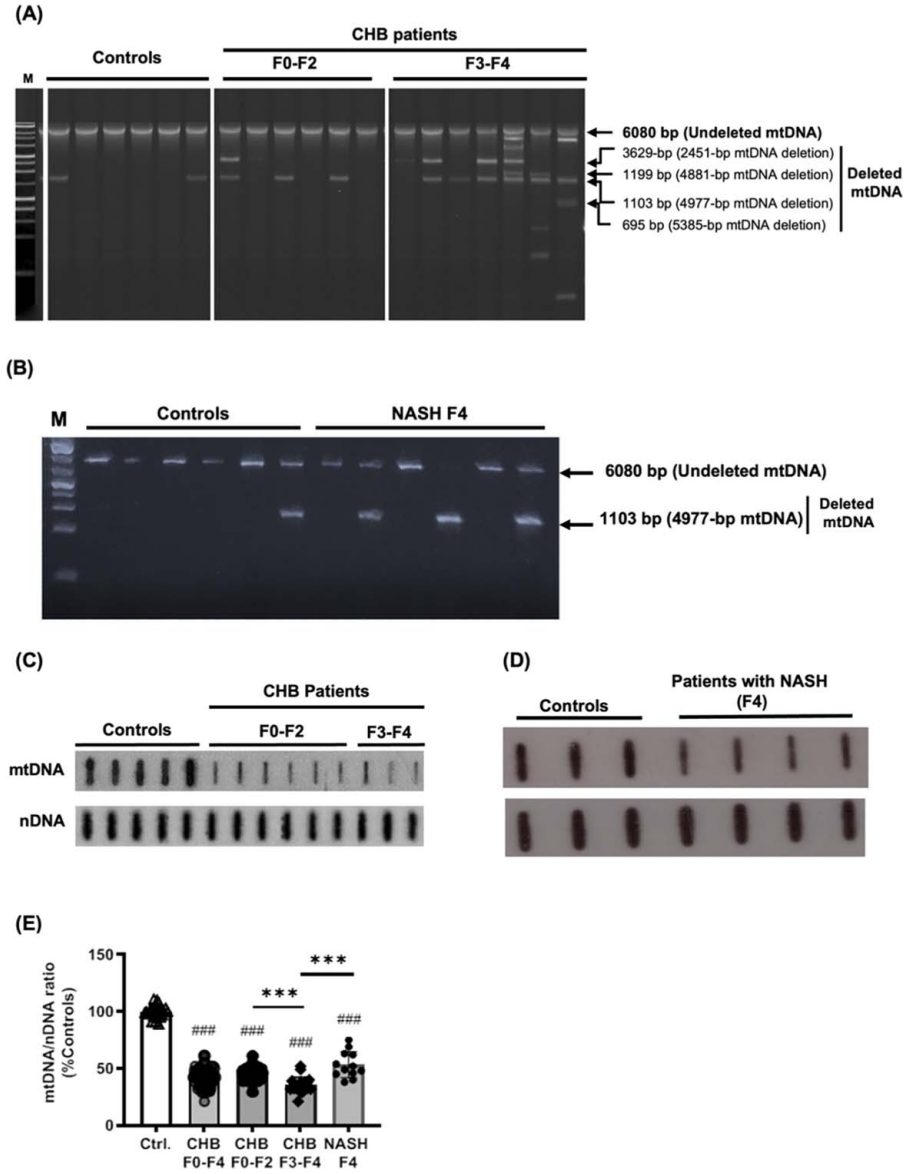

FIGURE 1 Liver mtDNA levels and mtDNA deletions. (A,B) Representative gels of LPCR detection of mtDNA deletions in controls, patients with CHB, and patients with NASH. In patients with CHB, primers A-B gave the 6080-bp product amplified from undeleted mtDNA and 3629-, 1199-, 1103-, or 695-bp products from deleted mtDNA (exact sizes were determined from the subsequently characterized 5385-, 4977-, 4881-, and 2451-bp mtDNA deletions in these patients) (A). In patients with NASH, the fragments of 1103-bp corresponding to the 4977-bp deletion was obtained (B). (C,D,E) Representative slot blottings (C,D) and mtDNA/nDNA ratios (mean ± SEM) from 65 patients with CHB (46 F0-F2 and 19 F3-F4) and 12 patients with NASH are expressed as percentages of 24 control values (E). M, 1 Kb DNA Ladder Plus. ###Different from control subjects, $p < 0.001$; ***Different from F0-F2 or from patients with NASH; $p < 0.001$, Mann–Whitney U test. Ctrl, controls. full color online

viral loads (HBV DNA: 6.0, 6.6, 7.2, 7.9, and 8.2 $\log_{10}$IU/ml). All 7 patients with NASH and with the 4977-bp deletion had massive steatosis (5 with 80% and 2 with 70% of fat-containing hepatocytes).

mtDNA levels in patients with CHB and patients with NASH

mtDNA levels were analyzed by slot blotting. nDNA levels were not modified when slot blottings were hybridized with the human C_0t-1 nDNA probe (Figure 1C,D). We thus used the mtDNA/nDNA hybridization ratio to quantitate mtDNA changes (Figure 1E). The mtDNA/nDNA ratio significantly declined in patients with CHB to 43% of control values ($p < 0.001$; Figure 1E). Compared to controls, the mtDNA/nDNA ratio significantly decreased by 55% in patients with CHB and F0-F2 ($p < 0.001$) and by 65% in patients with CHB and AF or cirrhosis ($p < 0.001$; Figure 1E).

Similarly, the mtDNA/nDNA ratio significantly declined to 53% of control values in patients with NASH and cirrhosis ($p < 0.001$; Figure 1E). The mtDNA/nDNA

ratio was also different when patients with CHB and F3-F4 were compared to patients with NASH and cirrhosis (35.37 ± 11.55 and 53.41 ± 11.55, respectively; $p < 0.001$).

Patients with CHB and highest viral loads (HBV DNA >5 $\log_{10}$IU/ml) all had the lowest mtDNA levels (mtDNA/nDNA ratio < 0.3). Similarly, patients with NASH and > 66% of steatosis had minimal mtDNA levels (mtDNA/nDNA ratios <0.5). Quantitative PCR confirmed mtDNA depletion in patients with CHB (Figure S3A).

We looked also for mtDNA strand breaks, topology, and changes in the main mtDNA forms in patients with CHB and controls (Figure S3B,C; see the Supporting Results section).

Exacerbated decreases in mtDNA-encoded cytochrome *c* oxidase subunits 1 and 2 in patients with CHB, CHC, or NASH and F3-F4 as compared to those with F0-F2

Compared to control livers ($n = 8$), mtDNA-encoded cytochrome *c* oxidase subunit 1 (MT-CO1) and mtDNA-encoded cytochrome *c* oxidase subunit 2 (MT-CO2) mRNA decreased significantly by 83% and 82% in patients with CHB and F3-F4 ($n = 21$), 70% and 61% in patients with CHC and F3-F4 ($n = 12$), and finally 65% and 59% in patients with NASH and cirrhosis ($n = 12$; $p < 0.001$; Figure 2A,C). Although significant, these decreases were, to a lesser extent, in patients with F0-F2 as compared to controls (Figure 2A,C).

MT-CO1 and MT-CO2 mRNA levels were then compared between F3-F4 and F0-F2 in patients with CHB or CHC. In patients with CHB and F3-F4 ($n = 21$), MT-CO1 mRNA (0.17 ± 0.11; $n = 21$) and MT-CO2 mRNA (0.18 ± 0.10; $n = 21$) decreased, respectively, by 53% and by 56% ($p < 0.001$) as compared to patients with F0-F2 (0.32 ± 0.24, $n = 66$ and 0.32 ± 0.22, $n = 66$; Figure 2A,B). In patients with CHC, MT-CO1 (F0-F2, $n = 21$; 0.61 ± 0.32 and F3-F4, $n = 12$; 0.30 ± 0.18) and MT-CO2 (F0-F2, $n = 21$; 0.64 ± 0.27 and F3-F4, $n = 12$; 0.39 ± 0.23) mRNA expression significantly decreased by 50% and 40% ($p < 0.001$), respectively, in patients with F3-F4 ($n = 12$) compared to those with F0-F2 ($n = 21$; Figure 2A,C).

We also observed a significant decrease ($p < 0.001$) in the expression of MT-CO2 mRNA, but not MT-CO1 mRNA, in patients with CHB and F3-F4 when compared

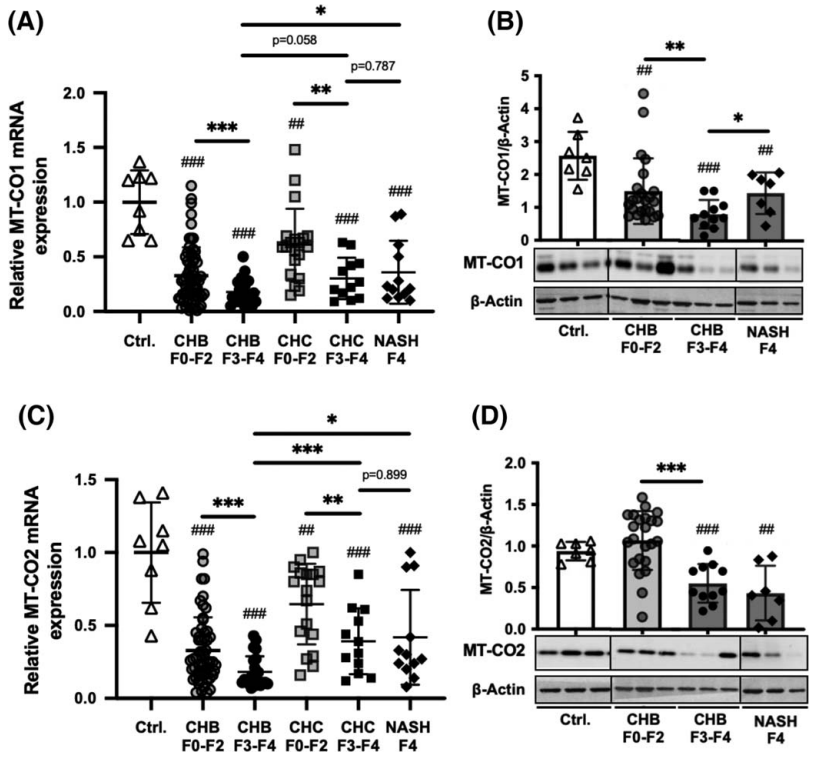

FIGURE 2 Liver mRNA and protein levels for mtDNA-encoded MT-CO1 and MT-CO2. (A,B) MT-CO1 mRNA and protein levels. MT-CO1 mRNA levels were compared in patients with CHB and F3-F4 ($n = 21$) or F0-F2 ($n = 66$), patients with CHC and F3-F4 ($n = 12$) or F0-F2 ($n = 12$), patients with NASH and cirrhosis ($n = 12$), and controls ($n = 8$) (A). MT-CO1 and β-Actin protein levels were assessed in patients with CHB and F3-F4 ($n = 11$) or F0-F2 ($n = 23$), patients with NASH and cirrhosis ($n = 7$), and controls ($n = 7$) (B). (C,D) MT-CO2 mRNA and protein levels. MT-CO2 mRNA levels were compared in patients with CHB and F3-F4 ($n = 21$) or F0-F2 ($n = 66$), patients with CHC and F3-F4 ($n = 12$) or F0-F2 ($n = 21$), patients with NASH and cirrhosis ($n = 12$), and controls ($n = 8$) (C). MT-CO2 and β-Actin protein levels were assessed in patients with CHB and F3-F4 ($n = 21$) or F0-F2 ($n = 11$), patients with NASH and cirrhosis ($n = 7$), and controls ($n = 7$) (D). Representative gels are shown. ##, ###Different from control subjects, ##$p < 0.01$, ###$p < 0.01$. *,**,***Different from F0-F2 or from patients with NASH; *$p < 0.05$, **$p < 0.01$, ***$p < 0.001$, Mann–Whitney U test. Ctrl, controls.

to patients with CHC and F3-F4 and a significant decrease in the expression of both MT-CO1 and MT-CO2 ($p < 0.05$) when patients with CHB and F3-F4 were compared to patients with NASH and cirrhosis (Figure 2A,C).

At the protein levels, the MT-CO1/β-Actin ratio significantly decreased in patients with CHB and F0-F2 (1.49 ± 1.01, $n = 23$; $p < 0.01$) or F3-F4 (0.81 ± 0.43, $n = 11$; $p < 0.001$) as compared to controls (2.56 ± 0.72, $n = 7$; Figure 2B). Compared to controls ($n = 7$), the MT-CO1/β-Actin and MT-CO2/β-Actin ratios were significantly decreased in patients with NASH and cirrhosis (1.45 ± 0.62 and 0.41 ± 0.32, respectively, $n = 7$; $p < 0.01$; Figure 2B,D).

Again, the decrease in the MT-CO1/β-Actin ($p < 0.01$) and MT-CO2/β-Actin ($p < 0.001$) ratios was worst in patients with CHB and F3-F4 ($n = 11$, 0.81 ± 0.43 and $n = 11$, 0.55 ± 0.23) than patients with CHB and F0-F2 (1.49 ± 1.01, $n = 23$ and 1.07 ± 0.35, $n = 21$). MT-CO1/β-Actin significantly decreased in CHB and F3-F4 as compared to those with NASH and cirrhosis (1.45 ± 0.61, $n = 7$; $p < 0.05$; Figure 2B).

However, nDNA-encoded cytochrome c oxidase subunit 4I1 (COX4I1) mRNA levels were unchanged in CHB and CHC whatever the degree of fibrosis, but significantly decreased in patients with NASH and cirrhosis as compared to control subjects ($p < 0.001$; Figure S4A). COX4I1 mRNA also significantly decreased in NASH and cirrhosis when compared to patients with CHB and F3-F4 ($p < 0.001$) or with CHC and F3-F4 ($p < 0.001$; Figure S4A).

Altered ^{mt}UPR in patients with CHB, patients with CHC, and patients with NASH

LONP1 degrades protein aggregates attributable to misfolding/disassembling of a surplus of mitochondrial proteins, whereas HSPA9 and HSPD1 allow respiratory chain complex assembly.[7]

Although expression of the ^{mt}UPR markers was altered in both patients with F0-F2 or with F3-F4, this alteration was more accentuated in patients with AF or cirrhosis associated with CHB or NASH (Figure 3).

LONP1 mRNA was induced in patients with CHB and with CHC whatever the degree of fibrosis, but this induction failed in patients with NASH and cirrhosis (Figure 3A). Compared to controls ($n = 8$), LONP1 mRNA levels significantly increased by 120% in patients with CHB and F0-F2 (2.20 ± 0.83, $n = 66$; $p < 0.001$), 65% in patients with CHB and F3-F4 (1.65 ± 0.56, $n = 18$; $p < 0.05$), and 140% in patients with CHC and F3-F4 (2.40 ± 1.03, $n = 11$; $p < 0.05$), but significantly decreased in patients with NASH and cirrhosis (0.18 ± 0.13, $n = 12$; $p < 0.001$; Figure 3A). Western blotting confirmed the induction of the LONP1 gene at the protein levels in patients with CHB and F0-F2 and, to a lesser extent, in F3-F4 (controls, $n = 7$; 0.23 ± 0.13 vs. CHB F0-F2, $n = 7$; 0.81 ± 0.29, $p < 0.01$ and vs. CHB F3-F4, $n = 6$; 0.52 ± 0.10, $p < 0.01$; Figure 3B).

Contrary to LONP1 mRNA, HSPA9 mRNA levels instead decreased significantly in patients with CHB or with NASH, but not in CHC, whereas HSPD1 mRNA significantly decreased in all these groups as compared to control subjects (Figure 3C,E).

In patients with CHB, LONP1 mRNAs levels significantly decreased in AF or cirrhosis (F3-F4, $n = 20$; 1.65 ± 0.56) as compared to those with F0-F2 ($n = 66$; 2.20 ± 0.83, $p < 0.05$; Figure 3A). Similarly, LONP1/β-Actin significantly decreased by 1.3-fold (F3-F4, $n = 6$; 0.52 ± 0.10 vs. F0-F2, $n = 7$; 0.82 ± 0.29, $p < 0.05$; Figure 3B).

Similarly, relative HSPA9 mRNA expression decreased significantly by 36% in patients with CHB and F3-F4 as compared to patients with CHB and F0-F2 (F3-F4, $n = 20$; 0.37 ± 0.19 and F0-F2, $n = 66$; 0.57 ± 0.23, $p < 0.001$; Figure 3C). This difference was confirmed by western blotting with a 1.7-fold significant decrease in patients with CHB and F3-F4 ($n = 10$; 0.57 ± 0.33) compared to those with F0-F2 ($n = 10$; 0.98 ± 0.25, $p < 0.01$; Figure 3D).

As compared to patients with CHB and F0-F2, HSPD1 mRNAs levels significantly decreased in patients with CHB and AF or cirrhosis (F3-F4, $n = 20$; 0.37 ± 0.17 and F0-F2, $n = 66$; 0.53 ± 0.24; $p < 0.05$; Figure 3E).

These differences in HSPA9 and HSPD1 mRNA expression were not observed between F3-F4 and F0-F2 within the group of patients with CHC (Figure 3C,E).

We finally compared patients with AF or cirrhosis within groups of CHB, CHC, and NASH. As compared to patients with CHB and F3-F4 or with CHC and F3-F4, LONP1 and HSPA9 mRNAs significantly decreased in patients with NASH and cirrhosis ($n = 12$; 0.18 ± 0.13, $p < 0.001$ and $n = 12$; 0.30 ± 0.20, $p < 0.001$, respectively; Figure 3A,C).

Mitophagy markers were induced in patients with CHB, CHC, or NASH, but this induction was altered during fibrosis progression in CHB

Expression of mitophagy markers was induced in patients with F0-F2 or F3-F4 whatever the etiology, but to a lesser extent in CHB and NASH patients with AF or cirrhosis (Figure 4). Compared to controls ($n = 8$; 1.00 ± 0.38), PRKN mRNA increased significantly by 144-fold in patients with F0-F2 ($n = 66$; 144.0 ± 54.3, $p < 0.001$) and by 45-fold in patients with F3-F4 ($n = 20$; 44.7 ± 20.2, $p < 0.001$) in the group of patients with CHB (Figure 4A). In patients with CHC, PRKN mRNA increased significantly by 35-fold in patients with

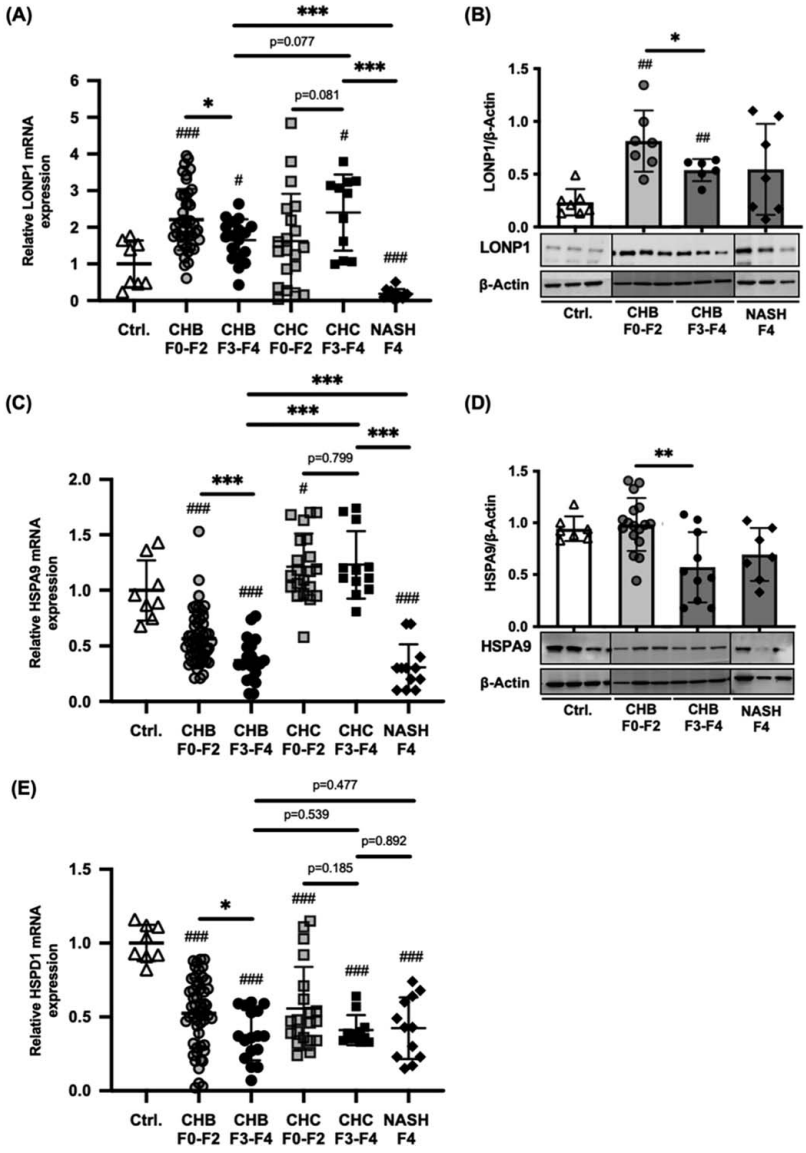

FIGURE 3 Evaluation of the mtUPR and mitophagy markers. (A) LONP1 mRNA levels were compared in patients with CHB and F3-F4 ($n = 18$) or F0-F2 ($n = 66$), patients with CHC and F3-F4 ($n = 11$) or F0-F2 ($n = 21$), 12 patients with NASH and F4, and 8 controls. (B) LONP1 protein levels were compared in patients with CHB and F3-F4 ($n = 7$) or F0-F2 ($n = 6$), 7 patients with NASH and F4, and 7 controls. (C) HSPA9 mRNA levels were compared in patients with CHB and F3-F4 ($n = 20$) or F0-F2 ($n = 66$), patients with CHC and F3-F4 ($n = 12$) or F0-F2 (n=21), 12 patients with NASH and F4, and 8 controls. (D) HSPA9 protein levels were compared in patients with CHB and F3-F4 ($n = 10$) or F0-F2 ($n = 17$), 7 patients with NASH and F4, and 7 controls. (E) HSPD1 mRNA levels were compared in patients with CHB and F3-F4 ($n = 20$) or F0-F2 ($n = 66$), patients with CHC and F3-F4 ($n = 11$) or F0-F2 ($n = 20$), 12 patients with NASH and F4, and 8 controls. $^{\#,\#\#,\#\#\#}$Different from controls ($p < 0.05$, 0.01, 001); *,**,***F3-F4 compared to F0-F2 within the same or between etiologies, $^{*}p < 0.05$, $^{**}p < 0.01$, $^{***}p < 0.001$, Mann–Whitney U test. Ctrl, controls.

F0-F2 ($n = 18$; 35.5 ± 25.1, $p < 0.001$) and by 115-fold in patients with F3-F4 ($n = 12$; 115.0 ± 64.2, $p < 0.001$) as compared to controls (Figure 4A). PRKN mRNA also increased significantly by 20-fold in patients NASH and cirrhosis ($n = 12$; 20.3 ± 11.4, $p < 0.001$) as compared to controls (Figure 4A). Compared to controls, induction of PRKN protein was confirmed in patients with CHB ($p < 0.001$) and in patients with NASH ($p < 0.01$; Figure 4B).

Similarly, PINK1 mRNA increased significantly by 4-fold in patients with F0-F2 ($n = 60$; 4.03 ± 1.12, $p < 0.001$) and by 1.9-fold in patients with F3-F4 ($n = 18$; 1.94 ± 0.53, $p < 0.001$) in the group of CHB as compared to controls ($n = 8$; 1.00 ± 0.50; Figure 4C). In patients with CHC, PINK1 mRNA increased significantly by 7-fold whatever the fibrosis stage (F0-F2, $n = 19$; 7.20 ± 3.25, $p < 0.001$ and F3-F4, $n = 12$; 7.11 ± 3.44, $p < 0.001$) as compared to control values (Figure 4C). PRKN and PINK1 mRNAs also increased significantly, by 20- and 1.3-fold, respectively, in patients with NASH and cirrhosis ($n = 12$; 20.3 ± 11.4, $p < 0.001$ and $n = 12$; 1.32 ± 0.75, $p < 0.001$) as compared to controls (Figure 4C). Induction

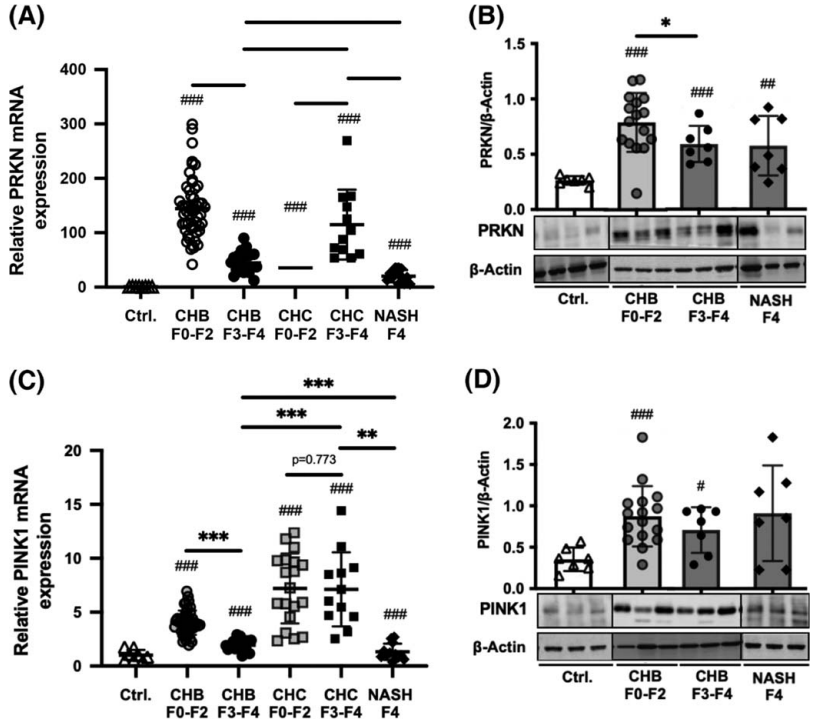

FIGURE 4 Expression of PRKN and PINK1 mRNA and proteins.(A) PRKN mRNA levels were compared in patients with CHB and F3-F4 ($n = 20$) or F0-F2 ($n = 66$), patients with CHC and F3-F4 ($n = 21$) or F0-F2 ($n = 12$), patients with NASH and F4 ($n = 12$), and controls ($n = 8$).(B) PRKN protein levels were compared in patients with CHB and F3-F4 ($n = 7$) or F0-F2 ($n = 12$), patients with NASH and F4 ($n = 7$), and controls ($n = 7$). (C) PINK1 mRNA levels were compared in patients with CHB and F3-F4 ($n = 18$) or F0-F2 ($n = 60$), patients with CHC and F3-F4 ($n = 12$) or F0-F2 ($n = 19$), patients with NASH and F4 fibrosis ($n = 12$), and controls ($n = 8$). (D) PINK1 protein levels were compared in patients with CHB and F3-F4 ($n = 7$) or F0-F2 ($n = 16$), patients with NASH and F4 ($n = 7$), and controls ($n = 7$). #,##,###Different from controls ($p < 0.05$, 0.01, 0.001); *,**,***F3-F4 compared to F0-F2 within the same or between etiologies, *$p < 0.05$, **$p < 0.01$, ***$p <$ 0,001, Mann–Whitney U test. Ctrl, controls.

of PINK1 protein was confirmed in patients with CHB and F0-F2 ($n = 16$; 0.88 ± 0.36, $p < 0.001$) and F3-F4 ($n = 7$; 0.71 ± 0.27, $p < 0.01$; Figure 4D).

In the group of patients with CHB, PRKN as well as PINK1 mRNAs significantly decreased, respectively, by 3.2-fold ($p < 0.001$) and 2.1-fold ($p < 0.001$) in patients with F3-F4 as compared to patients with F0-F2 (Figure 4A,C). PRKN protein expression also significantly decreased by 1.3-fold in patients with CHB and F3-F4 as compared to those with F0-F2 ($p < 0.05$; Figure 4B).

In the group of patients with CHC, a 3.2-fold increase in PRKN mRNA expression was observed in F3-F4 ($n = 12$; 115.0 ± 64.2) when compared to F0-F2 ($n = 19$; 35.5 ± 25.1, $p < 0.001$), whereas PINK1 mRNA remains unchanged whatever the fibrosis stage (Figure 4A,C).

When we compared AF or cirrhosis between these three groups, we noticed that PRKN and PINK1 mRNA expression significantly collapsed in patients with NASH and cirrhosis as compared to patients with CHB and F3-F4 ($p < 0.001$) or with CHC and F3-F4 ($p < 0.001$ and $p < 0.01$, respectively; Figure 4A,C).

In addition to the above analyzed markers for mitochondrial function, mitophagy, and ^{mt}UPR, we also investigated mRNA and/or protein levels for the mitochondrial biogenesis markers, PPARGC1α and TFAM (Figure S5), as well as the mitochondrial import marker, translocase of outer mitochondrial membrane 20 (TOMM20), which were all altered in patients with CHB, CHC, or NASH (Figure S5; see the Supporting Results section).

Decreased liver ATP levels and MT-ATP8 in patients with CHB

Liver ATP levels were 62% of control values in patients with CHB (0.5 ± 0.1 and 0.2 ± 0.1 μmole/mg of protein; $p < 0.05$; Figure 5A). A significant decrease of liver ATP was observed in patients with CHB and F3-F4 when compared to those with F0-F2 (0.1 ± 0.1 and 0.4 ± 0.2; $p < 0.01$; Figure 5A). Compared to control livers, expression of MT-ATP8 protein significantly decreased by 58% ($p < 0.01$) in patients with CHB whatever the degree of fibrosis (Figure 5B).

Increased iNOS protein but unchanged MnSOD protein expression in patients with CHB and F3-F4 when compared to patients with CHB and F0-F2

Compared to controls, iNOS protein, but not Manganese superoxide dismutase (MnSOD), significantly

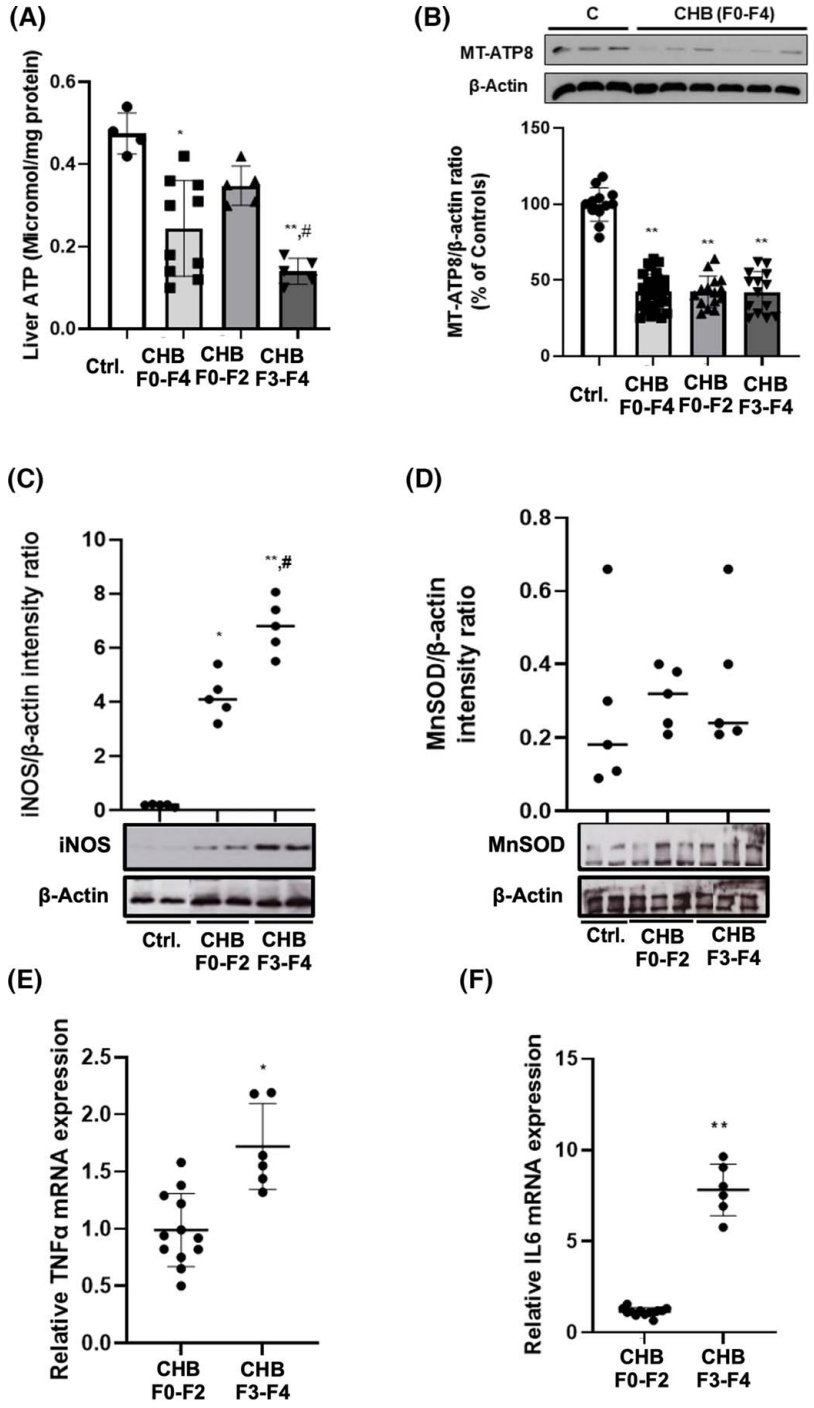

FIGURE 5 Liver ATP, MT-ATP8, iNOS, and MnSOD protein levels and liver mRNA of TNFα and IL6. (A) ATP levels were measured in four pools of 30-µg liver homogenates each obtained from 3 controls and 10 pools of 30-µg liver homogenates each obtained from 3 patients with CHB (5 pool F0-F2, 5 pool F3-F4). (B) Western blotting analysis for the MT-ATP8 subunit. MT-ATP8/β-Actin protein ratios (mean ± SEM) for 30 patients with CHB are expressed as the percentage of the mean of 12 control values. (C,D) Western blotting analysis for iNOS and MnSOD proteins and corresponding iNOS/β-actin and MnSOD/β-actin ratios from 5 controls, 5 F0-F2, and 5 F3-F4. Relative mRNA expression for TNFα (E) and IL6 (F) were determined by RT-qPCR in 6 patients with CHB F3-F4 and in 10 F0-F2 using specific primers. Different from controls, *$p < 0.05$; **$p < 0.01$. #Different from F0-F2, $p < 0.05$, Mann–Whitney U test.

increased in patients with CHB (Figure 5C,D). iNOS was also significantly induced in patients with F3-F4 compared to patients with F0-F2 (Figure 5C) whereas MnSOD remained unchanged in these two groups (Figure 5D).

Increased expression of liver TNFα and IL6 mRNAs in patients with CHB and F3-F4

Liver TNFα mRNAs were 1.72 ± 0.20 and 0.99 ± 0.20 ($p < 0.05$) and liver IL6 mRNAs were 7.82 ± 0.90 and

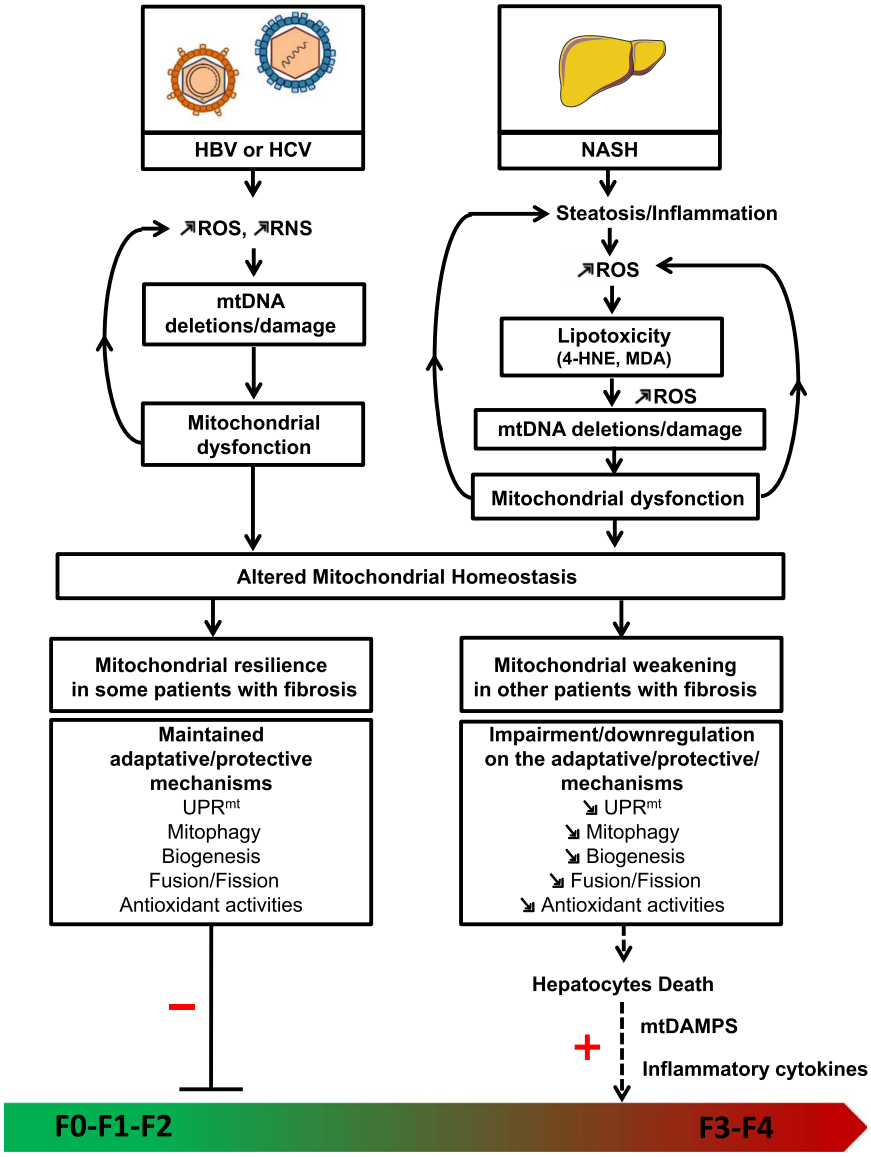

FIGURE 6 Suggested mechanisms for the role of mtDNA damage and mitochondrial stress in the progression of fibrosis. By depressing liver antioxidant capacities and partially blocking electron flow within the mitochondrial respiratory chain, HBV proteins or lipoperoxidation products malondialdehyde (MDA) and 4-hydroxynonenal (4-HNE) increase mitochondrial ROS formation, depress mitochondrial antioxidants, and favor hepatic OS. ROS and these lipotoxic intermediates then cause mtDNA damage. The replication of damaged mtDNA molecules leads to progressive accumulation of mtDNA deletions, resulting in profound mitochondrial dysfunction, which further increases ROS production and further mtDNA damage accumulation in a vicious cycle. ROS and mDAMPs also activate the proliferation and dedifferentiation of HSCs into myofibroblasts secreting collagens and fibrosis develops. In some patients, the mitochondrial resilience involving adaptive mechanisms (mtUPR, biogenesis, fusion, fission, and mitophagy) might maintain or restore mitochondrial homeostasis and limit ROS formation and liver inflammation. The fibrosis in this case stabilizes or regresses. However, in other patients, the altered mitochondrial mtUPR in combination with mitophagic burden lead to significant accumulation of extensively damaged mitochondria within infected or fat-engorged hepatocytes. Leakage of mtDNA and other mDAMPs in the cytosol could activate autocrine inflammatory responses. Alternatively, hepatocyte necrosis may lead to mDAMP release in the extracellular medium, leading to an activation of paracrine inflammatory responses in the neighboring hepatocytes, Kupffer cells, and resident macrophages. High ROS and inflammatory cytokines in this case could sustain mitochondrial stress, which may favor the progression of fibrosis.

1.14 ± 0.26 ($p < 0.05$) as assessed in 6 patients with CHB and F3-4 and 10 with F0-F2, respectively (Figure 5E,F). Liver IL1β mRNAs were comparable in both groups (1.04 ± 0.40 in F3-F4 and 1.24 ± 0.51 in F0-F2).

Similarly, expression of the mitochondrial fusion marker, MFN1, and the fission marker, OPA1, was altered in patients with CHB and F3-F4 (Figure S4; see the Supporting Results section).

Mitochondrial stress was also examined in HepG2 cells replicating HBV or expressing wild-type or mutated HBx proteins *in vitro* (Figures S6–S8, Tables S4 and S5; see the Supporting Results section).

DISCUSSION

The present study investigated the incidence of mtDNA damage and/or alterations in mitochondrial function and homeostasis in patients with CHB, CHC, and NASH and in healthy control subjects. We also compared patients with AF or cirrhosis (F3-F4) to patients with minimal/mild-moderate fibrosis (F0-F2). The study also explored *in vitro* the possible mechanisms involved in HBV-induced mitochondrial stress.

Four mtDNA deletions (5385-, 4977-, 4881-, and 2451-bp) associated with mtDNA depletion and mtDNA strand breaks were identified in patients with CHB (Figure 1, Figures S2 and S3). Only the 4977-bp deletion associated with mtDNA depletion was detected in NASH patients (Figure 1B). Expression of mtDNA-encoded MT-CO1, MT-CO2, and MT-ATP8 as well as liver ATP levels significantly decreased in patients with CHB when compared to healthy controls (Figures 2 and 6). Expression of mtDNA-encoded MT-CO1 and MT-CO2 also decreased in patients with NASH or CHC as compared to controls (Figure 2). Expression of the markers for ^{mt}UPR, mitophagy, and mitochondrial biogenesis all significantly altered in patients with AF or cirrhosis compared to patients with F0-F2 (Figures 3–6).

The 4977- and 5385-bp deletions, but not 4881- and 2451-bp, have been reported. The common 4977-bp mtDNA deletion is associated with normal age.[13,14] The 4977-bp and 5385-bp deletions have been reported in Wilson's disease and in alcoholics with microvesicular steatosis.[15,16] The mtDNA 4977-bp deletion has been reported also in NAFLDs,[30] HBV-related HCC,[31,32] as well as in a case of a CHB patient with toxic myopathy associated with long-term use of oral antiviral regiments.[33] Accumulation of oxidative mtDNA damage (mainly 8-hydroxydeoxyguanine) has been also reported in CHC.[34]

In patients with CHB, the higher prevalence and diversity of these mtDNA deletions were associated with AF or cirrhosis (Table S3). Fifty-six of 65 (86%) patients with CHB, including 30 of 46 (65%) patients with F0-F2 and 18 of 19 (95%) with F3-F4, had either one, two, or three different mtDNA deletions, whereas only 5 of 24 (21%) control subjects had a single mtDNA deletion (Table S3). In patients with NASH and cirrhosis, 7 of 12 (58%) presented a single 4977-bp mtDNA deletion (Table S3).

Subsequently, expression of mtDNA-encoded MT-CO1 and MT-CO2 was significantly decreased in F3-F4 when compared to F0-F2 (Figure 2). Expression of these mtDNA-encoded genes might be interpreted as the consequence of mtDNA deletions and lower mtDNA content detected in the present study, but also as a consequence of several other mtDNA point mutations including those described in the mtDNA regulatory sequence D-Loop in HBV-infected patients.[31,32,35] Point mutations in the D-Loop region might also explain the observed mtDNA depletion observed in our patients given that this sequence controls both transcription and replication of mtDNA.[11]

The mitophagy markers, PRKN and PINK1, as well as ^{mt}UPR markers HSPD1, HSPA9, and LONP1 or biogenesis marker TFAM were all down-regulated in patients with F3-F4 when compared to patients with F0-F2 (Figures 3 and 4, Figure S5). These mitochondrial lesions were associated with iNOS induction and liver inflammation in patients with CHB and F3-F4 (Figure 5). In addition to impaired mtDNA replication, mtDNA depletion might also be caused by mitophagy-mediated clearance of excessively damaged mitochondria.[7] mtDNA degradation occurred, to a different extent, in patients with F3-F4 as compared to those with F0-F2 (Figure 1, Figure S3), suggesting that the mitophagy process might be different in these patients. Accordingly, expression of the mitophagy markers, PINK1 and PRKN, significantly dropped in AF when compared to F0-F2, although they were induced in both groups as compared to controls (Figure 4).

Important possible mechanisms on the role of lipid peroxidation, mtDNA damage, and associated mitochondrial dysfunction in the development of liver steatosis in NASH and CHC were discussed (see the Supporting Discussion section).

HBV and HBx block electron flow within the respiratory chain and depressed mitochondrial antioxidant capacities, thus increasing ROS formation within mitochondria.[7,8,22,36,37] ROS-mediated mtDNA damage includes single- and double-strand breaks that favor slipped mispairing of repeated sequences during replication.[16,29,38,39] This may explain why the detected mtDNA deletions were all flanked by direct repeats in these patients (Figure S2A), consistent with a mechanism of slipped mispairing.[38,40] The higher frequency of the 4977-bp deletion in our patients may be explained by the long 13-bp direct repeats in this case favoring misannealing.

HBx has also been shown to interact with the mitochondrial voltage-dependent anion channel, consistent with its role in decreasing mitochondrial membrane potential and thus its increasing of the intracellular levels of ROS.[41] HBx interacted with B-cell lymphoma 2 (Bcl-2) and Bcl-2-extra large (Bcl-xL) to induce OS and cell death.[41] HBx containing G124L and I127A mutations prevented HBx binding to Bcl-2 and Bcl-xL and abrogated its role in opening MTP.[41] In the present study, mutated HBx(G124L, I127A) failed to increase mitochondrial OS, and failed to cause mtDNA depletion and complex I inactivation (Figure S8, Tables S4 and S5). Importantly, we have reported previously that specific protection against hepatocyte mitochondrial dysfunction plays a preventive role in early stages of fibrogenesis and delays its onset in transgenic mice specifically overexpressing Bcl-2 in

their hepatocytes.[42] Analyses of mtDNA, respiratory chain complexes, and lipid peroxidation showed that these Bcl-2 transgenic animals were protected against CCl_4-induced mitochondrial dysfunction and OS resulting in reduced fibrosis.[42]

Our data *in vitro* confirmed that HBV and HBx protein both induced a mitochondrial superoxide release (Figure S8A, Table S4). Superoxide itself is not only poorly reactive with biological compounds, but also it cannot cross biological membranes. However, it reacts with NO (formed within mitochondria or elsewhere) to form the highly reactive peroxynitrite.[17,19,20] Although the presence of iNOS within mitochondria is debated, the freely diffusible NO formed elsewhere can cross mitochondrial membranes to react with superoxide and form peroxynitrite within the mitochondria.[17] Indeed, iNOS is also highly expressed in peroxisomes, which are not only essential metabolic organelles with a central role in the synthesis and turnover of complex lipids, but also an important source of ROS, NO, and RNS.[43,44] Moreover, iNOS inhibited H_2O_2-scaveging peroxisomal catalase, leading to high hydrogen peroxide accumulation within this organelle, which may account for further hepatocellular damage through the lipotoxicity of lipid peroxidation by-products.[45] Thus, the combination of the increased mitochondrial superoxide formation (Figure S8A, Table S4) with the concomitant increased iNOS expression, wherever it took place (Figure 5, Figure S7), could markedly increase the mitochondrial formation of peroxynitrite in HBV-infected hepatocytes.

Peroxynitrite and/or peroxynitrite-generated reactive intermediates can damage mtDNA.[18–20] Overexpression of MnSOD, selective inhibition of iNOS, or peroxynitrite scavengers all attenuated mtDNA depletion in diverse situations.[18–20] iNOS inhibitor 1400 W and superoxide scavenger Mito-Tempo protected against HBx- and HBV-induced mtDNA depletion and respiratory complex I impairment (Table S5). Taken together, these observations suggest that the reaction of superoxide with NO to form the DNA-damaging peroxynitrite is involved in the mtDNA damage triggered by HBV.

Peroxynitrite also damages proteins, causing nitrotyrosine formation, tyrosine oxidation, and loss of function.[17,18] In the present study, HBV as well as HBx increased 3-nitrotyrosine residues in the proteins of mitochondrial complexes I, III, and V (Figure S7). Such nitration has been shown to decrease respiratory complex I activity,[17,18] to further enhance and sustain mitochondrial ROS formation.[7]

MnSOD is another target for ROS- and peroxynitrite-mediated inactivation.[18] Despite the induction of the MnSOD protein, MnSOD activity rather decreased in HepG2 cells after transfection with HBV or HBx, whereas Cu,ZnSOD activity remained unchanged (Figure S7). The reduced MnSOD activity in HBV-infected hepatocytes may further increase the intramitochondrial concentrations of superoxide and its reaction with NO to form peroxynitrite.

Thus, several redundant mechanisms may be involved in OS after HBV infection, including TNFα, respiratory chain impairment, decreased MnSOD activity, and induction of iNOS.

To preserve mitochondrial homeostasis, hepatocytes respond by inducing mitochondrial antioxidative capacities such as MnSOD, increasing mitochondrial fission to allow the mitophagy degradation of dysfunctional mitochondria, and increasing mitochondrial fusion and biogenesis to restore mtDNA levels and mitochondrial mass.[7,46] When these adaptive responses failed, hepatocytes then activated the protective ^{mt}UPR mechanisms through mitochondrial HSPA9 and HSPD1 to allow a correct folding of the mtDNA- and nDNA-encoded mitochondrial proteins.[7] The observed mtDNA damage in patients with CHB and NASH may cause the unbalance between these proteins of two genetic origins and lead to mitochondrial protein aggregates known to be toxic for mitochondria.[7] The mitochondrial peptidase, LONP1, then degrades the excess of imported mitochondrial proteins encoded by nDNA. Ultimately, hepatocytes might block the mitochondrial import of nDNA-encoded polypeptides and extensively damaged mitochondria cleaned by mitophagy in extreme situations. All these adaptive responses seem compromised in AF as shown by decreases in the expression of specific proteins, such as LONP1 peptidase and mitochondrial HSPA9 and HSPD1, required for proper ^{mt}UPR, PINK1, and PRKN involved in the mitophagy process (Figures 3 and 4) as well as TOMM20, MFN1, and OPA1 involved, respectively, in mitochondrial import, fusion, and fission (Figure S4). We noted, however, that mitophagy markers were induced in CHB and F0-F2, but this induction failed in F3-F4 (Figure 4).

Whatever the etiology, the above discussed mechanisms of oxidative mtDNA damage, mitochondrial dysfunction, and altered mitochondrial dynamics might all favor the development of fibrosis in several ways. First, the preexisting (inherited, acquired, or age-related) mtDNA deletions might aggravate the effects of HBV in CHB and the effects of lipoperoxidation products in NASH on mitochondrial function, which, in turn, might accelerate the development and progression of liver fibrosis. Patients with mtDNA deletions in the present study have developed hepatic fibrosis to a different extent. Those subjects, however, with multiple mtDNA deletions (and possibly many other mtDNA mutations) may produce more oxygen radicals and poorly eliminate ROS because of the altered mitochondrial antioxidant capacities.[7,47,48] This may lead to a marked increase in the lipid peroxidation products known to activate HSCs leading to collagen accumulation.[7] Patients with NASH and mtDNA

deletions and patients with CHC and mitochondrial dysfunction were all significantly older than patients with CHB and controls (Table 1). Unlike in the NASH group, where patients with mtDNA deletions were significantly older, the age of patients with mtDNA deletions and CHB was not different from the age of all other patients without the deletions in the present study. Similarly, the age of patients with CHB patients and AF was not different from the age of all other patients without mtDNA deletions. Thus, these observations excluded the effect of age on mtDNA in CHB and likely supported direct damaging effects of HBV on mtDNA in AF. Second, one cannot exclude that steatosis itself likely causes mtDNA damage and alters mitochondrial homeostasis. Steatosis and ROS favor the accumulation of lipid peroxidation products known to cause mtDNA damage, which may then favor the development of fibrosis. Lipohydroperoxides lead to mtDNA adducts and single-strand breaks and favor slipped mispairing of repeated sequences during replication of damaged mtDNA molecules, resulting in impaired oxidative phosphorylation, even though the percentage of mtDNA affected with these deletions is usually low.[13,22,49] This may be the case in NASH and CHC, but unlike in CHB. In NASH, massive steatosis associated with liver inflammation and OS lead to lipid peroxidation product hallmarks.[7] However, significant steatosis (thus lipid peroxidation) is a rare histological feature in our patients with CHB (Table 1) and other studies.[50–52] Third, altered mitophagy together with associated liver necrosis might favor the release of mitochondrial danger signals to induce the expression of inflammatory cytokines known to favor the development and progression of liver fibrosis.[7,9,53,54] Reduced mitophagy might thus promote immune and inflammatory responses through mitochondrial damage-associated molecular patterns (mDAMPs).[7,9,55–57] As such mDAMPs, mtDNA activates Toll-like receptor 9 and the NLRP3 inflammasome and leads to the expression and maturation of inflammatory cytokines.[7,55–61] Importantly, it has also been reported that mtDNA directly activates HSCs and collagen synthesis in mice fed a high-fat diet and in patients with NASH.[9] Finally, the observed effects of HBV may occur in liver residing in other cell types, including immune cells. HBV has been shown to cause mitochondrial dysfunction of HBV-specific CD8 T cells leading to their exhaustion and senescence.[62,63] In this case, mitochondrial dysfunction indirectly impairs the resolution of liver fibrosis attributable to the exhausted CD8 T and thus favors the progression of this lesion. Determining which of these hypotheses is correct clearly requires further studies.

Although the present study has several strengths (relevant knowledges for the understanding of the pathophysiology and mechanisms of chronic liver diseases), it also has several main limitations: First of all, there was our inability to simultaneously investigate all of the addressed parameters (RNA, DNA, and proteins) and characterize the intrahepatic HBV biomarkers (covalently closed circular DNA [cccDNA], 3.5-kb mRNAs, and the cccDNA transcriptional activity) in all samples because of the limited sizes of available biopsies. Second, the heterogeneity of different cell types (hepatocytes, inflammatory cells, and HSCs) has not been addressed. Third, the role of HBV-induced mitochondrial dysfunction in fibrosis progression needs further explorations. To this end, it will be of great interest to treat *in vitro* HSCs with purified mtDNA (as an mDAMP) or to coculture HBV-infected hepatocytes with HSCs and monitor their differentiation into collagen-secreting myofibroblasts and their expression of profibrogenic factors/markers. Studying mitochondrial stress in an HBV-infected liver humanized mouse model treated or not with CCl_4 would allow to explore the role of these mitochondrial lesions in the progression of fibrosis. Finally, experiments in other relevant models relying on HBV infection (with wild-type and HBx mutant viruses) are needed to confirm whether the mitochondrial alterations observed in our transfection system are induced by HBV replication and/or by other HBV proteins in addition to HBx.

We propose that mtDNA damage resulted in the disturbance of mitochondrial homeostasis, function, and dynamics in patients with CHB and patients with NASH. Suppressed ^{mt}UPR in combination with altered mitophagy leads to an overall significant mtDNA damage accumulation that subsequently increases mitophagic burden, leading to mDAMP release, and subsequent expression of inflammatory and profibrogenic mediators (Figure 6). All these mitochondrial alterations likely play important roles in triggering/exacerbating inflammatory and profibrotic responses that promote the development and progression of fibrosis (Figure 6).

Our observation that HBV- and HBx-induced mtDNA damage and mitochondrial dysfunction is preventable *in vitro* raises the hope that the dire prognosis of AF or cirrhosis could be therapeutically improved or slowed *in vivo*. Further investigations of the modulation of these potential mitochondrial biomarkers in large cohorts of patients with other liver diseases are urgently needed to confirm the feasibility of these markers for therapeutic and diagnosis purposes.

AUTHORS CONTRIBUTIONS

Concept, setup, and design (Abdellah Mansouri, Tarik Asselah); acquisition and analysis of data (Dimitri Loureiro, Abdellah Mansouri, Issam Tout, Cheikh Mohamed Bed, Morgane Roinard, Stéphanie Narguet, Ahmad Sleiman, and Tarik Asselah); writing original and final drafts (Abdellah Mansouri, Tarik Asselah, and Dimitri Loureiro); all authors were involved in critical

review of the manuscript and approved the final version of the manuscript.

FUNDING INFORMATION

This work was funded by INSERM and Université de Paris Cité.

CONFLICT OF INTEREST

Nothing to report.

ORCID

Dimitri Loureiro https://orcid.org/0000–0002–7860–8636
Issam Tout https://orcid.org/0000–0002–1019–3489
Vassili Soumelis https://orcid.org/0000–0003–1849–9834
Patrick Soussan https://orcid.org/0000–0003–2706–7371
Richard Moreau https://orcid.org/0000–0003–0862–403X
Valérie Paradis https://orcid.org/0000–0003–3142–3762
Abdellah Mansouri https://orcid.org/0000–0003–3856–5771

REFERENCES

1. Yuen MF, Tanaka Y, Fong DY, Fung J, Wong DK-H, Yuen JC-H, et al. Independent risk factors and predictive score for the development of hepatocellular carcinoma in chronic hepatitis B. J Hepatol. 2009;50:80–8.
2. Foerster F, Galle PR. Comparison of the current international guidelines on the management of HCC. JHEP Rep. 2019;1:114–9.
3. Bedossa P, Poynard T. An algorithm for the grading of activity in chronic hepatitis C. The METAVIR Cooperative Study Group. Hepatology. 1996;24:289–93.
4. Asselah T, Loureiro D, Boyer N, Mansouri A. Targets and future direct-acting antiviral approaches to achieve hepatitis B virus cure. Lancet Gastroenterol Hepatol. 2019;4:883–92.
5. Terrault NA, Lok ASF, McMahon BJ, Chang K-M, Hwang JP, Jonas MM, et al. Update on prevention, diagnosis, and treatment of chronic hepatitis B: AASLD 2018 hepatitis B guidance. Hepatology. 2018;67:1560–99.
6. Wei C, Ni C, Song T, Liu Y, Yang X, Zheng Z, et al. The hepatitis B virus X protein disrupts innate immunity by downregulating mitochondrial antiviral signaling protein. J Immunol. 2010;185:1158–68.
7. Mansouri A, Gattolliat CH, Asselah T. Mitochondrial dysfunction and signaling in chronic liver diseases. Gastroenterology. 2018;155:629–47.
8. Hossain MG, Akter S, Ohsaki E, Ueda K. Impact of the interaction of hepatitis B virus with mitochondria and associated proteins. Viruses. 2020;12:175.
9. An P, Wei LL, Zhao S, Sverdlov DY, Vaid KA, Miyamoto M, et al. Hepatocyte mitochondria-derived danger signals directly activate hepatic stellate cells and drive progression of liver fibrosis. Nat Commun. 2020;11:2362.
10. Acerbi G, Montali I, Ferrigno GD, Barili V, Schivazappa S, Alfieri A, et al. Functional reconstitution of HBV-specific CD8 T cells by in vitro polyphenol treatment in chronic hepatitis B. J Hepatol. 2021;74:783–93.
11. Anderson S, Bankier AT, Barrell BG, de Bruijn MH, Coulson AR, Drouin J, et al. Sequence and organization of the human mitochondrial genome. Nature. 1981;290:457–65.
12. Holt IJ, Lorimer HE, Jacobs HT. Coupled leading- and lagging-strand synthesis of mammalian mitochondrial DNA. Cell. 2000;100:515–24.
13. Cortopassi G, Wang E. Modelling the effects of age-related mtDNA mutation accumulation; complex I deficiency, superoxide and cell death. Biochim Biophys Acta. 1995;1271:171–6.
14. Ames BN, Shigenaga MK, Hagen TM. Oxidants, antioxidants, and the degenerative diseases of aging. Proc Natl Acad Sci U S A. 1993;90:7915–22.
15. Mansouri A, Gaou I, Fromenty B, Berson A, Lettéron P, Degott C, et al. Premature oxidative aging of hepatic mitochondrial DNA in Wilson's disease. Gastroenterology. 1997;113:599–605.
16. Mansouri A, Fromenty B, Berson A, Robin MA, Grimbert S, Beaugrand M, et al. Multiple hepatic mitochondrial DNA deletions suggest premature oxidative aging in alcoholic patients. J Hepatol. 1997;27:96–102.
17. Choumar A, Tarhuni A, Lettéron P, Reyl-Desmars F, Dauhoo N, Damasse J, et al. Lipopolysaccharide-induced mitochondrial DNA depletion. Antioxid Redox Signal. 2011;15:2837–54.
18. Mansouri A, Tarhuni A, Larosche I, Reyl-Desmars F, Demeilliers C, Degoul F, et al. MnSOD overexpression prevents liver mitochondrial DNA depletion after an alcohol binge but worsens this effect after prolonged alcohol consumption in mice. Dig Dis. 2010;28:756–75.
19. Larosche I, Lettéron P, Berson A, Fromenty B, Huang T-T, Moreau R, et al. Hepatic mitochondrial DNA depletion after an alcohol binge in mice: probable role of peroxynitrite and modulation by manganese superoxide dismutase. J Pharmacol Exp Ther. 2010;332:886–97.
20. Cover C, Mansouri A, Knight TR, Bajt ML, Lemasters JJ, Pessayre D, et al. Peroxynitrite-induced mitochondrial and endonuclease-mediated nuclear DNA damage in acetaminophen hepatotoxicity. J Pharmacol Exp Ther. 2005;315:879–.
21. Ivanov AV, Valuev-Elliston VT, Tyurina DA, Ivanova ON, Kochetkov SN, Bartosch B, et al. Oxidative stress, a trigger of hepatitis C and B virus-induced liver carcinogenesis. Oncotarget. 2017;8:3895–932.
22. Ling LR, Zheng DH, Zhang ZY, Xie W-H, Huang Y-H, Chen Z-X, et al. Effect of HBx on inflammation and mitochondrial oxidative stress in mouse hepatocytes. Oncol Lett. 2020;19:2861–9.
23. Lee SY, Choi YM, Oh SJ, Yang S-B, Lee J, Choe W-H, et al. rt269I Type of Hepatitis B Virus (HBV) Leads to HBV e Antigen Negative Infections and Liver Disease Progression via Mitochondrial Stress Mediated Type I Interferon Production in Chronic Patients With Genotype C Infections. Front Immunol. 2019;10:1735.
24. Liang YJ, Teng W, Chen CL, Sun CP, Teng RD, Huang YH, et al. Clinical implications of HBV PreS/S mutations and the effects of PreS2 deletion on mitochondria, liver fibrosis, and cancer development. Hepatology. 2021;74:641–55.
25. Gao WY, Li D, Cai DE, Huang XY, Zheng BY, Huang YH, et al. Hepatitis B virus X protein sensitizes HL-7702 cells to oxidative stress-induced apoptosis through modulation of the mitochondrial permeability transition pore. Oncol Rep. 2017;37:48–56.
26. Huang C, Shao J, Lou C, Wu F, Ge T, Gao H, et al. Reduced energy metabolism impairs T cell-dependent B cell responses in patients with advanced HBV-related cirrhosis. Front Immunol. 2021;12:660312.
27. Lin YT, Liu W, He Y, Wu YL, Chen WN, Lin XJ, et al. Hepatitis B Virus X Protein Increases 8-Oxo-7,8-Dihydro-2′-Deoxyguanosine (8-Oxodg) Level via Repressing MTH1/ MTH2 Expression in Hepatocytes. Cell Physiol Biochem. 2018;51:80–96.
28. Asselah T, Bièche I, Laurendeau I, Martinot-Peignoux M, Paradis V, Vidaud D, et al. Significant gene expression differences in histologically “Normal” liver biopsies: implications for control tissue. Hepatology. 2008;48:953–62.
29. Mansouri A, Gaou I, De Kerguenec C, Amsellem S, Haouzi D, Berson A, et al. An alcoholic binge causes massive degradation

of hepatic mitochondrial DNA in mice. Gastroenterology. 1999; 117:181–90.
30. Kamfar S, Alavian SM, Houshmand M, Yadegarazari R, Seifi Zarei B, Khalaj A, et al. Liver mitochondrial DNA copy number and deletion levels may contribute to nonalcoholic fatty liver disease susceptibility. Hepat Mon. 2016;16:e40774.
31. Gwak GY, Lee DH, Moon TG, Choi MS, Lee JH, Koh KC, et al. The Correlation of Hepatitis B Virus Pre-S Mutation with Mitochondrial D-loop Mutations and Common Deletions in Hepatocellular Carcinoma. Hepatogastroenterology. 2011;58:522–8.
32. Wheelhouse NM, Lai PBS, Wigmore SJ, Ross JA, Harrison DJ. Mitochondrial D-loop mutations and deletion profiles of cancerous and noncancerous liver tissue in hepatitis B virus-infected liver. Br J Cancer. 2005;92:1268–72.
33. Fujii T, Takase KI, Honda H, Kawamura N, Yamasaki R, Urata M, et al. Toxic myopathy with multiple deletions in mitochondrial DNA associated with long-term use of oral anti-viral drugs for hepatitis B: a case study. Neuropathology. 2019;39:162–7.
34. Fujita N, Sugimoto R, Ma N, Tanaka H, Iwasa M, Kobayashi Y, et al. Comparison of hepatic oxidative DNA damage in patients with chronic hepatitis B and C. J Viral Hepat. 2008;15:498–507.
35. Lee HC, Li SH, Lin JC, Wu CC, Yeh DC, Wei YH. Somatic mutations in the D-loop and decrease in the copy number of mitochondrial DNA in human hepatocellular carcinoma. Mutat Res. 2004;547:71–8.
36. Rahmani Z, Huh KW, Lasher R, Siddiqui A. Hepatitis B virus X protein colocalizes to mitochondria with a human voltage-dependent anion channel, HVDAC3, and alters its transmembrane potential. J Virol. 2000;74:2840–6.
37. Khan M, Syed GH, Kim SJ, Siddiqui A. Hepatitis B virus-induced parkin-dependent recruitment of linear ubiquitin assembly complex (LUBAC) to mitochondria and attenuation of innate immunity. PLoS Pathog. 2016;12:e1005693.
38. Cortopassi GA, Shibata D, Soong NW, Arnheim N. A pattern of accumulation of a somatic deletion of mitochondrial DNA in aging human tissues. Proc Natl Acad Sci U S A. 1992;89:7370–4.
39. Wallace DC. Mitochondrial genetic medicine. Nat Genet. 2018; 50:1642–9.
40. Trinh TQ, Sinden RR. The influence of primary and secondary DNA structure in deletion and duplication between direct repeats in Escherichia coli. Genetics. 1993;134:409–22.
41. Geng X, Huang C, Qin Y, McCombs JE, Yuan Q, Harry BL, et al. Hepatitis B virus X protein targets Bcl-2 proteins to increase intracellular calcium, required for virus replication and cell death induction. Proc Natl Acad Sci U S A. 2012;109:18471–6.
42. Mitchell C, Robin MA, Mayeuf A, Mahrouf-Yorgov M, Mansouri A, Hamard M, et al. Protection against hepatocyte mitochondrial dysfunction delays fibrosis progression in mice. Am J Pathol. 2009;175:1929–37.
43. Loughran PA, Stolz DB, Vodovotz Y, Watkins SC, Simmons RL, Billiar TR. Monomeric inducible nitric oxide synthase localizes to peroxisomes in hepatocytes. Proc Natl Acad Sci U S A. 2005; 102:13837–42.
44. Ding L, Sun W, Balaz M, He A, Klug M, Wieland S, et al. Peroxisomal β-oxidation acts as a sensor for intracellular fatty acids and regulates lipolysis. Nat Metab. 2021;3:1648–61.
45. Kono Y, Fridovich I. Superoxide radical inhibits catalase. J Biol Chem. 1982;257:5751–4.
46. Gammage PA, Moraes CT, Minczuk M. Mitochondrial genome engineering: the revolution may not be CRISPR-Ized. Trends Genet. 2018;34:101–10.
47. Gehring A, Bertoletti A, Tavis JE. Host factor-targeted hepatitis B virus therapies. Intervirology. 2014;57:158–62.
48. Shirakata Y, Koike K. Hepatitis B virus X protein induces cell death by causing loss of mitochondrial membrane potential. J Biol Chem. 2003;278:22071–8.
49. Lee YI, Hwang JM, Im JH, Lee YI, Kim NS, Kim DG, et al. Human hepatitis B virus-X protein alters mitochondrial function and physiology in human liver cells. J Biol Chem. 2004;279: 15460–71.
50. Xu D, Liu L, Zhao Y, Yang L, Cheng J, Hua R, et al. Melatonin protects mouse testes from palmitic acid-induced lipotoxicity by attenuating oxidative stress and DNA damage in a SIRT1-dependent manner. J Pineal Res. 2020;69:e12690.
51. Zhong GC, Wu YL, Hao FB, Rao XW, Yuan XW, Zhao Y, et al. Current but not past hepatitis B virus infection is associated with a decreased risk of nonalcoholic fatty liver disease in the Chinese population: a case-control study with propensity score analysis. J Viral Hepat. 2018;25:842–52.
52. Worland T, Apostolov R, Asadi K, Leung C. Hepatitis B virus activity is not associated with degree of liver steatosis in patients with hepatitis B-related chronic liver disease. Liver Int. 2020;40: 1500–2.
53. Bueno M, Lai YC, Romero Y, Brands J, St Croix CM, Kamga C, et al. PINK1 deficiency impairs mitochondrial homeostasis and promotes lung fibrosis. J Clin Invest. 2015;125:521–38.
54. Zhong Z, Umemura A, Sanchez-Lopez E, Liang S, Shalapour S, Wong J, et al. NF-κB restricts inflammasome activation via elimination of damaged mitochondria. Cell. 2016;164:896–910.
55. Zhong Z, Liang S, Sanchez-Lopez E, He F, Shalapour S, Lin X-J, et al. New mitochondrial DNA synthesis enables NLRP3 inflammasome activation. Nature. 2018;560:198–203.
56. Zhang Q, Raoof M, Chen Y, Sumi Y, Sursal T, Junger W, et al. Circulating mitochondrial DAMPs cause inflammatory responses to injury. Nature. 2010;464:104–7.
57. Tout I, Loureiro D, Mansouri A, Soumelis V, Boyer N, Asselah T. Hepatitis B surface antigen seroclearance: immune mechanisms, clinical impact, importance for drug development. J Hepatol. 2020;73:409–22.
58. Marques PE, Amaral SS, Pires DA, Nogueira LL, Soriani FM, Lima BHF, et al. Chemokines and mitochondrial products activate neutrophils to amplify organ injury during mouse acute liver failure. Hepatology. 2012;56:1971–82.
59. Garcia-Martinez I, Santoro N, Chen Y, Hoque R, Ouyang X, Caprio S, et al. Hepatocyte mitochondrial DNA drives nonalcoholic steatohepatitis by activation of TLR9. J Clin Invest. 2016;126:859–64.
60. Riley JS, Tait SW. Mitochondrial DNA in inflammation and immunity. EMBO Rep. 2020;21:e49799.
61. Rodríguez-Nuevo A, Díaz-Ramos A, Noguera E, Díaz-Sáez F, Duran X, Muñoz JP, et al. Mitochondrial DNA and TLR9 drive muscle inflammation upon Opa1 deficiency. EMBO J. 2018;37: e96553.
62. Scozzi D, Cano M, Ma L, Zhou D, Zhu JH, O'Halloran JA, et al. Circulating mitochondrial DNA is an early indicator of severe illness and mortality from COVID-19. JCI Insight. 2021;6:143299.
63. Fisicaro P, Barili V, Montanini B, Acerbi G, Ferracin M, Guerrieri F, et al. Targeting mitochondrial dysfunction can restore antiviral activity of exhausted HBV-specific CD8 T cells in chronic hepatitis B. Nat Med. 2017;23:327–6.

How to cite this article: Bed CM, Roinard M, Sleiman A, Boyer N, Pons-Kerjean N, Castelnau C, et al. Mitochondrial stress in advanced fibrosis and cirrhosis associated with chronic hepatitis B, chronic hepatitis C, or nonalcoholic steatohepatitis. Hepatology. 2023;77:1348–1365. https://doi.org/10.1002/hep.32731